https://doi.org/10.5194/egusphere-2025-3845
Preprint. Discussion started: 4 December 2025


# Chemical Precursors to Wintertime Carbonyl and Ozone Formation

Loknath Dhar[1,2], Seth N. Lyman[1,2]

[1]Department of Chemistry and Biochemistry, Utah State University, Logan, UT 84322, USA
[2]Bingham Research Center, Utah State University, Vernal, UT 84078, USA

*Correspondence to:* Seth Lyman (seth.lyman@usu.edu)

**Abstract**: Using the Framework for 0-D Atmospheric Modeling (F0AM), a zero-dimensional box model designed for simulating atmospheric chemistry, we simulated winter $O_3$ formation in the Uinta Basin, Utah, with four chemical mechanisms: the Master Chemical Mechanism (MCMv331), Statewide Air Pollution Research Centre Mechanism (SAPRC07), Regional Atmospheric Chemistry Mechanism (RACM2), and Carbon Bond Mechanism (CB6). Our purpose was to (1) identify key carbonyl precursors that act as important precursors to winter $O_3$ formation and determine how they form, (2) determine the extent to which carbonyl compounds were primarily or secondarily produced, (3) assess $O_3$ production potential, and (4) analyze how different hydrocarbon groups influence both carbonyl and $O_3$ formation. The final emission flux for carbonyls was near zero, indicating that they were mostly secondary photochemical products. MCMv331 identified formaldehyde and acetaldehyde as the dominant $O_3$ precursors, contributing 0.20 and 0.06 ppb/h, respectively, to the $O_3$ production rate. SAPRC07 and RACM2 showed similar trends, while CB6 emphasized the generic group "ketones" as key contributors. Across all mechanisms, alkanes were the most influential precursor group for the formation of carbonyls and $O_3$. Including heterogeneous chemistry in the model resulted in a modest (1 ppb) decrease in $O_3$ levels without altering the relative importance of precursors. This study highlights the importance of primarily emitted organic groups in winter $O_3$ production and provides insights into $O_3$ reduction strategies in the Uinta Basin and similar regions.

## 1. Introduction

Elevated tropospheric $O_3$ levels have raised serious concerns over the past decades due to their harmful effects on human health and the environment. High ground-level $O_3$ can cause respiratory issues, eye irritation, and chest discomfort (Soares et al., 2022; Filippidou et al., 2011). It also negatively impacts ecosystems (Ashmore et al., 2000) and contributes to climate change in the long term (Barnes et al., 2019; Simpson et al., 2014). Tropospheric $O_3$ forms through photochemical reactions involving precursors like nitrogen oxides (NOx) and non-methane organic compounds (NMOC) and is highly influenced by meteorological and topographical conditions. Although tropospheric $O_3$ is typically considered a summertime problem, high $O_3$ during winter conditions has been reported worldwide. Notable examples include Wyoming, USA (2008) and Lanzhou, China (2018), where high $O_3$ levels were observed despite cold winter conditions (Yang et al., 2024). Weak vertical mixing and high NMOC mixing ratios existed in all of these cases. Mansfield and Hall (2018) and Mansfield and Lyman (2024) showed that wintertime $O_3$ can only form in high-NMOC environments (Mansfield et al., 2018; Mansfield et al., 2024).

https://doi.org/10.5194/egusphere-2025-3845
Preprint. Discussion started: 4 December 2025


In the Uinta Basin, Utah, USA, high levels of ground-level $O_3$ were initially observed in December 2009, drawing attention to wintertime $O_3$ pollution in the region (Mansfield et al., 2020). This phenomenon is primarily attributed to a combination of strong temperature inversions with snow cover and emissions from oil and gas operations. Geographically, the Uinta Basin is surrounded by high mountains, creating a bowl-shaped terrain that traps local pollution. This topography provides ideal conditions for creating strong thermal inversions that form at the lowest elevations and expand daily until disrupted by a significant storm (Lyman et al., 2015; Oltmans et al., 2014). Snow cover plays an important role in stabilizing inversions by reducing the mixed-layer height (Edward et al., 2014). Snow cover also increases the surface albedo, which leads to a higher actinic flux for photolysis reactions (Mansfield et al., 2013). Under these conditions, precursors emitted from oil and gas operations accumulate in the basin and undergo photochemical reactions in the presence of sunlight to produce $O_3$, and $O_3$ itself accumulates day after day (Lyman et al., 2015).

The photochemical process starts with the reaction of hydroxyl (OH) radicals with hydrocarbons, forming alkyl radicals (R1). These radicals rapidly react with oxygen to form peroxy radicals (R2), which, in the presence of nitrogen monoxide (NO), convert into alkoxy radicals while generating nitrogen dioxide ($NO_2$) (R3). The $NO_2$ then undergoes photolysis (R4), producing an oxygen atom that reacts with molecular oxygen to form $O_3$ (R5) (Wilkes, 2020).

In this whole process, radicals play a crucial role in initiating and sustaining the oxidation cycles of $O_3$ production by driving the interaction between NMOC and NOx in the troposphere (Carter et al., 2012; Seinfeld et al., 1989).

$$\bullet OH + CH_4 \rightarrow \bullet CH_3 + H_2O \qquad R1$$
$$\bullet CH_3 + O_2 + M \rightarrow CH_3O_2\bullet + M \qquad R2$$
$$CH_3O_2\bullet + NO\bullet \rightarrow CH_3O\bullet + NO_2 \qquad R3$$
$$NO_2 + h\nu \rightarrow NO\bullet + \bullet O \qquad R4$$
$$\bullet O + O_2 + M \rightarrow O_3 + M \qquad R5$$

During the summer, radicals mostly come from the photolysis of $O_3$ and the subsequent reaction of $O(^1D)$ with water vapor (Levy, 1971). However, this mechanism becomes less efficient in winter due to decreased ultraviolet light and water vapor, leading to a 15-to-60-fold reduction in primary radical production (Lehi et al., 1971; Edward et al., 2013). Photolysis of carbonyl compounds and other photolabile oxygenated NMOC (ONMOC) is another source of radicals that can lead to $O_3$ production (Carbajo et al., 2008). These carbonyls can originate from the oxidation of primarily emitted, non-oxygenated NMOC (as shown in R6 through R8). In the Uinta Basin, the winter conditions and the high mixing ratio of NMOC originating from oil and gas operations enhance the role of carbonyl photolysis as the dominant source of oxidants (Edward et al., 2014).

$$CH_3O\bullet + O_2 \rightarrow HCHO + HO_2\bullet \qquad R6$$

https://doi.org/10.5194/egusphere-2025-3845
Preprint. Discussion started: 4 December 2025


$HCHO + h\nu + O_2 \rightarrow 2\ HO_2\bullet + CO$ R7

$3\ (HO_2\bullet + NO\bullet \rightarrow OH\bullet + NO_2)$ R8

Radical amplification is a chemical process in which a small number of atmospheric radicals (OH or $HO_2$) initiate reaction chains that generate additional radicals, greatly increasing their overall mixing ratio. In the sequence of reactions R1, R2, R3, R6, R7, and R8, this chain leads to the formation of three OH radicals from a single initial OH, demonstrating the multiplying effect of radical amplification and showing how a high-NMOC wintertime atmosphere can still produce adequate radicals for significant $O_3$ production. These unique and complex interactions between geographical, meteorological, and chemical conditions create an ideal environment for winter $O_3$ formation in the Uinta Basin.

Previous studies on $O_3$ pollution have primarily focused on the relationship between $O_3$ and its precursors during the summertime (Yang et al., 2024). However, studies such as Edwards et al. (2014) highlight the important role of carbonyl compounds in winter, emphasizing their contribution to radical production and subsequent $O_3$ formation. Despite this progress, the detailed chemical mechanisms driving winter $O_3$ events remain underexplored. Addressing this knowledge gap is critical for understanding the unique conditions driving winter $O_3$ production in regions like the Uinta Basin.

A zero-dimensional (0-D) box model like the Framework for 0-D Atmospheric Modeling (F0AM) simplifies the atmosphere into a single, well-mixed "box," isolating chemical processes from transport effects, which allows controlled experimentation with precursor emissions and environmental parameters, enabling a detailed analysis of chemical processes. It is also capable of simulating winter-specific conditions such as low temperatures, limited sunlight, and stagnant boundary layers, which makes it ideal for studying winter $O_3$ formation (Wolfe et al., 2016). Researchers have previously utilized F0AM to simulate wintertime $O_3$ (Lyman et al., 2022, and Mansfield et al., 2024).

In this study, we investigated the chemistry of carbonyl compounds and a number of primarily emitted organic compounds, focusing on their role in winter $O_3$ formation in the Uinta Basin. Using the F0AM box model and the MCMv331, we examined the sensitivity of primarily emitted organic groups (alkane, alkene, alkyne, alcohol, and aromatic groups) in the formation of carbonyl compounds and their overall impact on winter $O_3$ production. The MCM is a near-explicit chemical mechanism that represents detailed gas-phase degradation of various NMOC, resulting in the formation of $O_3$ and other secondary pollutants (Saunders et al., 2003). To establish a solid understanding of the chemical processes driving winter $O_3$ formation, we compared the outputs of MCMv331 with lumped mechanisms, including the RACM2, SAPRC07, and CB6. Our goal in these comparisons was to identify a chemical mechanism that balances computational efficiency with chemical accuracy for future 3D photochemical modeling.

## 2. Method

### *2.1 Site Description and Study Period*

https://doi.org/10.5194/egusphere-2025-3845
Preprint. Discussion started: 4 December 2025


We acquired measurement data for this study at the Horsepool atmospheric monitoring station, located in the central Uinta Basin, Utah, at 40.143°N latitude and 109.469°W longitude, at an elevation of 1569 meters above sea level. This remote desert site is far removed from urban emissions and is primarily influenced by nearby oil and gas operations, making it an ideal location for investigating the impacts of these activities on regional air quality and wintertime $O_3$ formation. (Lyman et al., 2015; Neemann et al., 2015; Mansfield et al., 2020).

The simulation period (24–27 February 2019) was notable for a strong thermal inversion and the buildup of winter $O_3$. These inversion episodes were characterized by persistent snow cover from January through early March 2019, which contributed to multiday stagnation episodes and the accumulation of $O_3$ near the surface. The inversion layer acted as a barrier, limiting vertical mixing and trapping $O_3$ precursors close to the ground, thereby enhancing local photochemical $O_3$ production (Lyman et al., 2022).

### *2.2 Instrumentation*

We measured trace gases at the Horsepool site by pulling air through an unheated PTFE filter pack inlet into an indoor PFA manifold at 10 L min$^{-1}$. We used the Ecotech analyzer models 9810, 9841, 9843, and 9830 to measure $O_3$, $NO_x$, $NO_y$, and CO, respectively; the Chromatotec Chroma THC Analyzer to measure the methane and total nonmethane hydrocarbons; and the Met One BAM 1020 to measure $PM_{2.5}$. We utilized the Ecotech GasCal and Thermo 701H zero air generator to perform weekly calibrations. We recorded meteorological parameters, including snow depth (MaxBotix MB7092), total solar radiation (Kipp and Zonen CNR4), wind speed and direction (RM Young 05108-45-L), temperature and humidity (Vaisala HMP155), and barometric pressure (Vaisala PTB101B), with a Campbell CR1000 Datalogger, which we checked annually against NIST-traceable standards (Lyman et al., 2022).

We also measured speciated nonmethane organic compounds, including C2−C10 hydrocarbons, C1−C3 alcohols, and 12 carbonyl compounds, (carbonyl measurements were not available for 2019, so average values from inversion periods in other seasons were used) (Lyman et al., 2022). We collected air samples in silonite-coated whole-air canisters for hydrocarbons and alcohols and on DNPH (2,4-dinitrophenylhydrazine) cartridges for carbonyls. We collected one 3-hour sample daily, alternating start times between midnight and noon. We analyzed the collected DNPH cartridge samples by eluting the absorbed carbonyl compounds from the DNPH cartridges using a mixture of 75% acetonitrile and 25% dimethyl sulfoxide. Afterward, we injected those samples into a high-performance liquid chromatography (HPLC) system with a UV detector to separate, identify, and quantify the carbonyl-DNPH derivatives based on their retention times and peak areas. More details can be found in Lyman et al. (Lyman et al., 2020). We preconcentrated whole-air canister samples with an Entech 7200 using a cold-trap dehydration method and analyzed them by gas chromatography with flame ionization detection for C1−C3 hydrocarbons and by gas chromatography-mass spectrometry for the other compounds. (Lyman et al., 2022; Lyman et al., 2020).

### *2.3 Box Model*

https://doi.org/10.5194/egusphere-2025-3845
Preprint. Discussion started: 4 December 2025


We used the Framework for 0-D Atmospheric Modeling (F0AM) box model version 4.1 (Wolfe et al., 2016; Xiong et al., 2023) with a setup of an average diurnal cycle to simulate winter $O_3$ production, similar to Lyman et al. (2022). We utilized the average hourly meteorological data, CO, and total nitrogen oxides ($NO_x$) from the 4-day modeling period as the input for each individual modeled day (The model determined the $NO_x$ speciation). Model input included the study-period average mixing ratio of all organic compounds, including methane and individual hydrocarbons, alcohols, and carbonyls. We applied an albedo of 0.7 for winter, which aligned with observations over the study period, and used an $O_3$ column of 275 Dobson units, based on data from the OMI satellite (OMDOAO3e v003), obtained via NASA's Giovanni application (NASA Giovanni, 2024). We employed the same variable boundary layer heights followed by Edwards et al. (2014). We also started with the same variable dilution constant (kdil) as Edwards et al., but we adjusted the constant until $O_3$ was similar to observed values, following Ninneman et al. (2023).

We used a subset of the master chemical mechanism version 3.3.1 (MCMv331) (Saunders et al., 2003; Bloss et al., 2005), consisting of 3423 chemical species and 10309 chemical reactions. This explicit mechanism addressed the processes involved in the formation and breakdown of all measured organic compounds, including reaction rates, radical formation, and the propagation and amplification of other chemical factors influencing winter $O_3$ production.

For a subset of model runs, we also introduced heterogeneous chemistry to understand the impact on winter $O_3$ formation due to OH and $HO_2$ uptake onto the aerosol surface, following the method of Ninneman et al. (2023).

### *2.4 Comparison with Lumped Chemical Mechanisms*

We compared MCMv331 with several lumped mechanisms that consist of fewer species and reactions, including the Regional Atmospheric Chemistry Mechanism version 2 (RACM2), the Statewide Air Pollution Research Center Chemical Mechanism version 07 (SAPRC07), and the Carbon Bond Chemical Mechanism version 6 (CB6). Lumped mechanisms simplify atmospheric chemical modeling by aggregating similar species and reactions into fewer representative categories, which reduces computational complexity and enhances efficiency, making them ideal for large-scale air-quality models. Lumped mechanisms allow for faster computation while still capturing essential chemical processes, which is very important for the computational efficiency of large 3-D photochemical models. (Zaveri et al., 1999).

To compare these mechanisms, we conducted species mapping to aggregate and convert measured organic chemical species into the corresponding species in the lumped mechanisms. We used species properties in the United States Environmental Protection Agency (EPA) SPECIATE database version 5.2, along with a species conversion database provided by Ramboll (EPA, 2024). The conversion database is included in the Supplementary Information. When more than one MCM species matched a single lumped mechanism species, we aggregated their mixing ratios as appropriate.

### *2.5 Emission Flux*

https://doi.org/10.5194/egusphere-2025-3845
Preprint. Discussion started: 4 December 2025


Hydrocarbons in the Uinta Basin are primarily emitted from oil and gas activity (Lyman et al., 2015; Mansfield et al., 2020; Warneke et al., 2014), and because our hydrocarbon dataset was limited temporally, we set their mixing ratios to a constant value throughout the simulation period. In contrast, carbonyl compounds can be emitted directly or secondarily through photochemical reactions of hydrocarbons. To accurately simulate atmospheric conditions and allow for realistic secondary carbonyl production in the model, we created optimized emission flux (EF) for carbonyls. We set initial mixing ratios to measured values but allowed mixing ratios to vary in subsequent modeled hours. We iteratively adjusted the EF values to achieve mixing ratios with a minimal increasing or decreasing trend across the four model days. If the Day 4 mixing ratio for a carbonyl compound lay below the Day 1 value, the initial EF was too low, and we increased it incrementally until the lines aligned to the extent possible. Conversely, if the mixing ratios increased throughout the simulation, the EF was too high, and we reduced it, sometimes to zero. An EF of zero implied no local emissions and that all carbonyls, except those initially present, were formed from atmospheric photochemical reactions (Maasakkers et al., 2019). By systematically adjusting the EF values, we ensured the modeled mixing ratios of carbonyl compounds accurately reflected observed atmospheric behavior, thereby enhancing the reliability of the simulation results.

### *2.6 Determination of the Influence of Selected Carbonyls on $O_3$ Production*

To investigate the influence of a particular carbonyl compound on winter $O_3$ production, we initially ran the F0AM Box model without any modifications to observe the baseline $O_3$ production. We then set the initial mixing ratio of a specific carbonyl compound to zero and forced it to remain at zero while running the model again. Next, we compared the average $O_3$ production rate (ppb/h) between 9:00 and 16:00 on the 4th day of the simulation in both scenarios. We chose this timeframe (9:00 to 16:00) to ensure consistent photochemical activity when carbonyls participate in radical production during daylight, contributing to $O_3$ formation (Pang et al., 2006). The changes in $O_3$ production rate, when the mixing ratio of a specific carbonyl compound was forced to zero, allowed us to quantify its influence. We systematically repeated this process for all measured carbonyls and compared the outputs to determine compound-specific contributions to $O_3$ production.

### *2.7 Determination of the Influence of Primarily Emitted Organics on Carbonyl and $O_3$ Production*

We conducted a sensitivity analysis of the impacts of primarily emitted organic groups (alkanes, alkenes, alkynes, alcohols, and aromatics) on carbonyl production. We performed the sensitivity analysis for selected carbonyl compounds, including formaldehyde, acetaldehyde, methacrolein, benzaldehyde, and methyl ethyl ketone, chosen based on their significant impact on winter $O_3$ formation. We varied the initial mixing ratios of primary organic groups by ±50% (while keeping speciation within the group the same) and observed the corresponding percentage changes in the average mixing ratios of carbonyls between 13:00 and 17:00 on the fourth day of the simulation. We chose this timeframe to avoid the rapid changes in boundary layer height that occur in the morning, which could introduce variability in pollutant mixing ratio (Lapworth, 2006; Mahrt, 1981). During the afternoon period, the atmosphere is more homogeneous, allowing for an even distribution of precursors and reaction products. It also represents a steady-state condition for radical species (•OH, •$HO_2$, and •$RO_2$), ensuring a balanced production and loss cycle (Lew et al.,

https://doi.org/10.5194/egusphere-2025-3845
Preprint. Discussion started: 4 December 2025


2020; Heard et al., 2004). This approach allowed us to evaluate the sensitivity of carbonyl formation to fluctuations in levels of primary organic groups.

We also performed a similar sensitivity analysis to determine the influence of primarily emitted organic groups on the $O_3$ production rate, which allowed us to identify the individual impact of each organic compound group on winter $O_3$ production.

## 3. Results and Discussion

### *3.1 Winter $O_3$ Pollution in the Uinta Basin*

Figure S1 represents the diurnal variation of the hourly average $O_3$ mixing ratio during the simulation period in the Uinta Basin. On the fourth day, the daily maximum 8-h average $O_3$ mixing ratio reached 94 ppb, exceeding the U.S. Environmental Protection Agency standard of 70 ppb; The maximum hourly value was 102 ppb. The negative relationship between $O_3$ and relative humidity is shown in Fig. S2. In comparison, the F0AM Box model with the explicit chemical mechanism MCMv331 estimated a maximum $O_3$ mixing ratio of 107 ppb on the fourth day of the simulation (Fig. 1). After incorporating heterogeneous chemistry based on MCMv331, the $O_3$ level decreased by 1 ppb. The SAPRC07 lumped mechanism estimated the $O_3$ level at 111 ppb, while RACM2 predicted slightly lower than the measured value at 100 ppb, and CB6 provided the highest estimation of 122 ppb. Liu et al. (2023) conducted a Box model study with commonly used chemical mechanisms during summertime in China and identified that RACM2 showed the best agreement with observation during the polluted period, followed by MCMv331 and SAPRC07. These findings aligned with our study. On the other hand, Shareef et al. (2022) evaluated different lumped chemical mechanisms with CMAQ (3D photochemical model) on winter $O_3$ prediction and found no significant differences in SAPRC07, RACM2, and CB6 output.

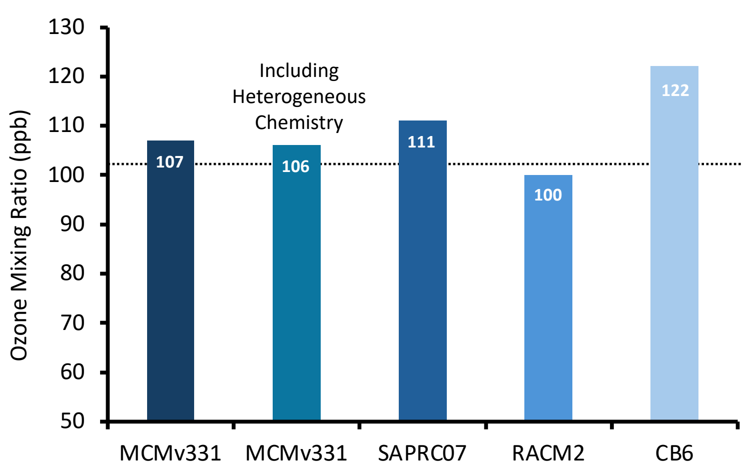

https://doi.org/10.5194/egusphere-2025-3845
Preprint. Discussion started: 4 December 2025


**Figure 1: Comparative analysis of maximum hourly $O_3$ mixing ratio using different chemical mechanisms. The dotted line represents the observed maximum hourly $O_3$ level (102 ppb).**

*3.2 Contribution of Carbonyls to Winter $O_3$ Formation*

Figure 2 shows that $O_3$ was more sensitive to changes in carbonyl mixing ratios in the lumped mechanisms compared to MCMv331. Master Chemical Mechanism (MCM) employs an explicit representation of reactions, wherein carbonyl compounds degrade through multi-generational, branched pathways that distribute radical formation across several intermediate species and slower reaction steps (Saunders et al., 2003). On the other hand, with simplified chemical mechanisms, carbonyl chemistry is formulated to produce $O_3$ forming radicals like $HO_2$ rapidly and directly, often in a single reaction step. This fundamental difference in mechanism structure may explain the higher $O_3$ sensitivity to carbonyls observed with the lumped mechanisms compared to MCMv331 (Goliff et al., 2013; Yarwood et al., 2010).

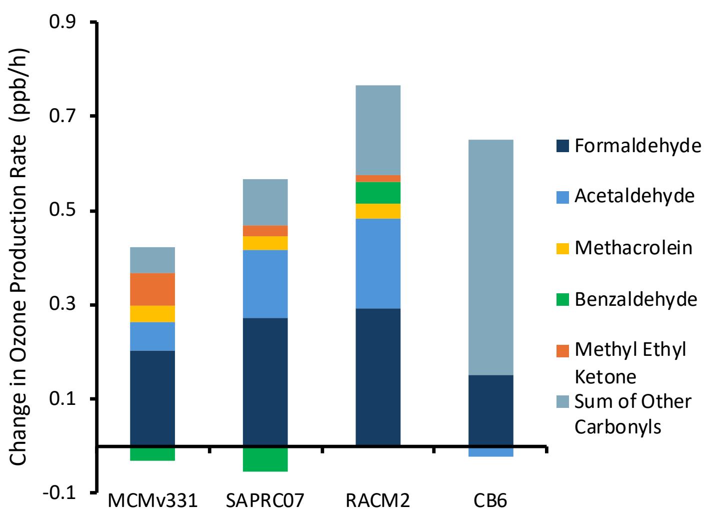


**Figure 2: Change in $O_3$ production rate on Day 4 of the modeled period in response to a 50% increase in the mixing ratio of the indicated carbonyls. Each bar represents the overall change in $O_3$ production rate for a specific chemical mechanism. The sections within each bar illustrate the contributions of individual carbonyl compounds.**

The F0AM box model with MCMv331 identified formaldehyde as the dominant contributor to the $O_3$ production rate, accounting for a change of 0.20 ppb/h, or approximately 50% of the total contribution from carbonyl compounds. This finding aligns with Edwards et al. (2014), who reported formaldehyde as the primary daytime radical source in the Uinta Basin, contributing 30% of radical formation from carbonyls, with the remainder attributed to larger carbonyl

https://doi.org/10.5194/egusphere-2025-3845
Preprint. Discussion started: 4 December 2025


species. In MCMv331, acetaldehyde was the second-highest contributor in our study, causing a change of 0.06 ppb/h in the $O_3$ production rate, with SAPRC07 and RACM2 following a similar trend. The MCMv331 mechanism showed that benzaldehyde had a negative contribution of -0.03 ppb/h, indicating that an increase in benzaldehyde mixing ratio in the system leads to a reduction in $O_3$ production rate. Benzaldehyde is treated as a simplified $HO_2$ source in the RACM2 and CB6 mechanisms (Goliff et al., 2013; Yarwood et al., 2010), contributing positively or neutrally to $O_3$ production. However, in MCMv331 and SAPRC07, benzaldehyde undergoes more detailed aromatic degradation involving peroxy radicals and secondary oxygenates that may consume radicals or produce less reactive species (Saunders et al., 2003; Carter, 2010). As a result, benzaldehyde competes for OH and acts as a radical sink, leading to a negative impact on the $O_3$ production rate in these more explicit mechanisms. This behavior is also supported by the radical budgets in Tables S10.1–S10.4. In MCMv3.3.1 and SAPRC07, the reaction OH + benzaldehyde represents a meaningful fraction of the total hydrogen oxide radicals (HOx) loss, so adding more benzaldehyde increases radical termination and lowers both OH and $HO_2$ levels. This reduction in radicals suppresses the NO–$NO_2$ cycling that drives ozone formation, leading to a negative $O_3$ response. In contrast, in RACM2 the flux through OH + BALD (benzaldehyde) is much smaller relative to the total HOx budget (less than 1%). As a result, increasing benzaldehyde does not significantly increase HOx loss. At the same time, RACM2 treats BALD photolysis as an efficient $HO_2$ source, so the added benzaldehyde actually produces more radicals than it removes. The net gain in HOx enhances NO oxidation and leads to a positive $O_3$ production response.

In CB6, most medium and high molecular weight carbonyls are lumped into the single "KET" species (Yarwood et al., 2010), so KET represents a much larger carbon pool than any individual carbonyl. As shown in Table S10.4, almost all KET is formed through the alkoxy-radical pathway (ROR → KET, ~99%), which strongly promotes radical propagation. At the same time, formaldehyde in CB6 undergoes a substantial $HO_2$ removal reaction (FORM + $HO_2$, ~31% of its loss; Table S10.4), limiting its radical yield. As a result, KET has a much stronger effect on $O_3$ production than formaldehyde in CB6.

The relative contributions of each carbonyl compound remained largely unchanged after introducing heterogeneous chemistry into the model (Fig. S4). This is likely due to low specific humidity during the simulation period, which limits the uptake of HOx radicals by aerosols. As a result, the radical budget and hence $O_3$ production potential were not significantly altered (Fig. 1), preserving the dominance of formaldehyde and acetaldehyde among carbonyl precursors.

Edwards et al. (2014) attributed 85% of radical production to the photolysis of carbonyl compounds during a 2013 winter $O_3$ episode at the same Uinta Basin location. However, studies have shown that the emissions in the Uinta Basin have declined since the Edwards et al. study (Mansfield et al., 2020; Lin et al., 2021), and during our study, we found that the initial mixing ratios of several carbonyls were lower compared to those of Edwards et al. on the fourth day of the simulation period (Table S1). Furthermore, the emission flux required to simulate representative carbonyl mixing ratios was minimal or zero. The addition of carbonyl emissions in the box model led to an overestimation of their mixing ratios, indicating that carbonyls were mostly secondary pollutants, created in the atmosphere from

https://doi.org/10.5194/egusphere-2025-3845
Preprint. Discussion started: 4 December 2025


photochemistry, rather than emitted directly from sources. Stockwell et al. (2011) and Nogueira et al. (2017) also identified carbonyl compounds mainly as secondary pollutants generated through the oxidation of hydrocarbons from anthropogenic or biogenic emissions.

### *3.3 Contribution of Hydrocarbons to Carbonyl Compound Formation*

Figure 3 illustrates the contribution of various hydrocarbon groups to the formation of key carbonyl compounds, including alkanes, alkenes, alkynes, aromatics, and alcohols. The MCMv3.3.1 results indicated that formaldehyde formation is influenced by a wide variety of NMOC groups (Fig. 3), which is also relatable to the abundance of NMOC species (Table S3). Among the various NMOC classes, the ozonolysis of alkenes and aromatic compounds is a notable pathway for formaldehyde formation (Saunders et al., 2003). While alkanes are generally less reactive than alkenes, due to their prominent mixing ratio in the atmosphere, they still play a dominant role in the formation of carbonyl compounds. Alkanes react with OH radicals to form peroxy radicals, which subsequently convert into alkoxy radicals in the presence of NO (Reactions R1–R3). These alkoxy radicals can then undergo β-scission, leading to the formation of carbonyl compounds, including formaldehyde (Wilkes, 2020; Rauk et al., 2003). The mixing ratios of acetaldehyde, benzaldehyde, and methyl ethyl ketone increased by 24%, 28%, and 20%, respectively, in response to a 50% increase in the initial mixing ratio of total alkanes. Methacrolein showed the largest response, with an 83% increase. In contrast, a 50% increase in aromatics led to a 9% decrease in methacrolein production.

Alkanes appeared as the most important precursor (causing a 28% increase) compared to aromatics in benzaldehyde formation, which contradicts what may be the traditional viewpoint. Studies have shown, however, that alkanes can undergo extensive autoxidation under high atmospheric mixing ratios (Crounse et al., 2013; Wang et al., 2021; Edward et al., 2014). As illustrated in reactions R1–R3, alkane species are initially converted into alkoxy radicals. These radicals can then undergo intramolecular cyclization, forming stable 5- and 6-membered ring structures (Nozière et al., 2024). Continued oxidation of these cyclic intermediates can ultimately lead to the formation of aromatic compounds and, subsequently, aromatic-containing carbonyls such as benzaldehyde. Tables S3–S7 show the percent change in carbonyl compound formation resulting from ±50% changes in the initial mixing ratios of individual NMOC, based on MCMv331 outputs. The ambient mixing ratios in the tables highlight how the abundance of certain NMOC species, primarily light alkanes, affects the formation of various carbonyl compounds, even though their reactivity is relatively low.

https://doi.org/10.5194/egusphere-2025-3845
Preprint. Discussion started: 4 December 2025


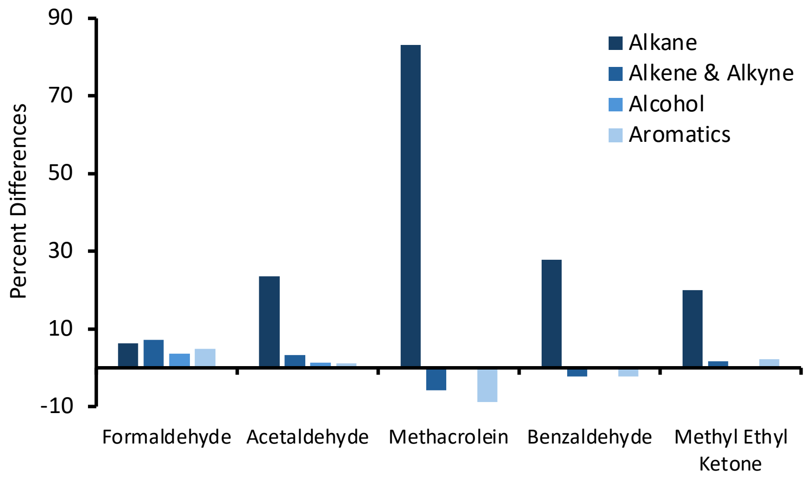


**Figure 3: Sensitivity of carbonyl compounds to changes in NMOC precursor groups (MCMv331 output). The bars represent the changes in carbonyl mixing ratios due to an increase in the NMOC mixing ratio of 50%.**

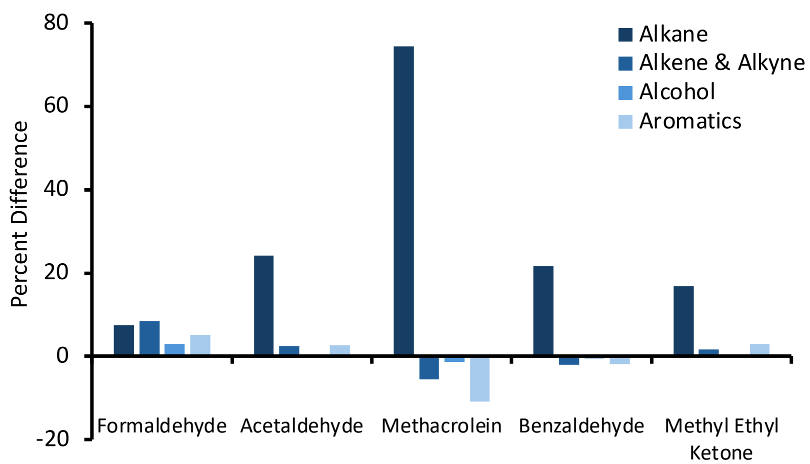


**Figure 4: Sensitivity of hydrocarbons to carbonyl compounds (SAPRC07 Output). The bars represent the changes in carbonyl mixing ratios to the increase in hydrocarbon initial mixing ratio by 50%.**

https://doi.org/10.5194/egusphere-2025-3845
Preprint. Discussion started: 4 December 2025


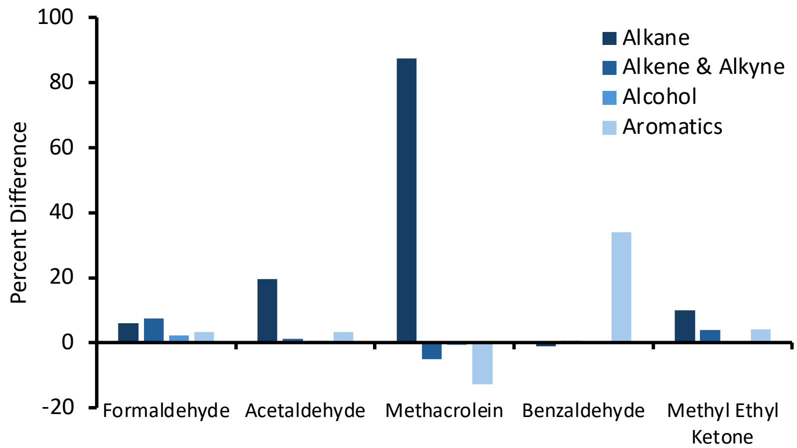


**Figure 5: Sensitivity of hydrocarbons to carbonyl compounds (RACM2 Output). The bars represent the changes in carbonyl mixing ratios to the increase in hydrocarbon initial mixing ratio by 50%.**

Sensitivity analyses following the same method with the SAPRC07 and RACM2 (Fig. 4 and 5) chemical mechanisms showed similar trends as MCMv331, except aromatics had a more substantial positive effect on benzaldehyde formation than alkanes, according to RACM2. As the CB6 mechanism is based on chemical bonds rather than actual chemical species, it provides significantly different results in terms of the impacts of hydrocarbons on formaldehyde production compared to the other three mechanisms (Fig. 6). The contribution of the different NMOC groups to acetaldehyde formation was nearly the same as the other chemical mechanisms, however. Alkanes acted as a major contributor to the formation of other carbonyls (KET in the CB6 mechanism) compared to other hydrocarbons. Figures S6–S9 show that a 50% decrease in the mixing ratios of each NMOC group resulted in similar magnitudes of change in carbonyl mixing ratios, but in the opposite direction.

https://doi.org/10.5194/egusphere-2025-3845
Preprint. Discussion started: 4 December 2025


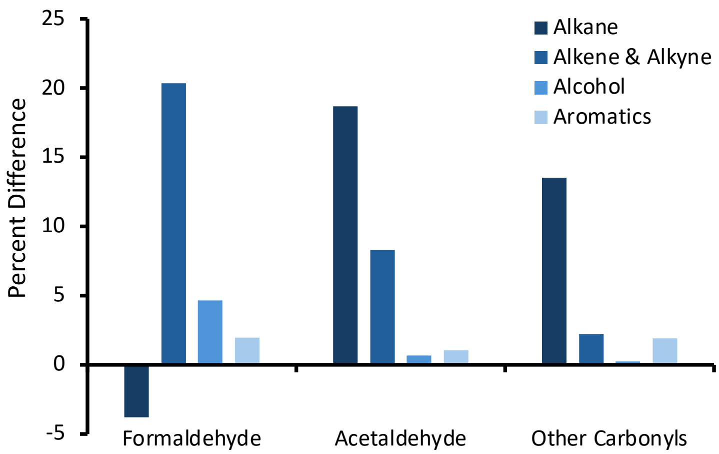


**Figure 6: Sensitivity of hydrocarbons to carbonyl compounds (CB6 Output). The bars represent the changes in carbonyl mixing ratios to the increase in hydrocarbon initial mixing ratio by 50%.**

### *3.4 Contribution of Hydrocarbons to Winter $O_3$ Formation*

To elucidate the impact of various hydrocarbons on winter $O_3$ formation and gain deeper insights into the underlying chemistry, we conducted a sensitivity analysis using the same chemical mechanisms as before. Figure 7 reveals that both MCMv331 and SAPRC07 chemical mechanisms exhibit similar chemical behavior, with alkanes having the most significant influence on winter $O_3$ formation. A 50% increase in the mixing ratio of alkanes resulted in approximately a 0.29 ppb/h and 0.35 ppb/h increase in $O_3$ production rate on the fourth day of the simulation with the MCMv331 and SAPRC07 mechanisms, respectively.

Aromatics emerged as the second most important precursors for MCMv331 and SAPRC07. Simulations conducted using the RACM2 mechanism showed that alkanes and aromatics had nearly similar contributions to the $O_3$ production rate. The CB6 mechanism identified alkanes as the major contributor, similar to MCMv331 and SAPRC07. However, it ranked alkenes and alkynes, rather than aromatics, as the second-highest contributors to winter $O_3$ production, diverging from the trends observed in the other chemical mechanisms.

These box model results show that emissions of alkanes from oil and gas extraction play a critical role in wintertime $O_3$ formation (Chen et al., 2020; Koss et al., 2015). In Utah's Uintah Basin, light alkanes are the most abundant in NMOC (Table S2). Although light alkanes react more slowly with OH radicals compared to aromatics, they dominate the NMOC mix by volume and account for around 70% of OH-initiated hydrocarbon oxidation, making them key $O_3$ precursors in the Uinta Basin, according to Koss et al. (2015). Other studies in oil and gas-producing areas have found that light alkanes contribute about 60% of OH reactivity on average and significantly aid in forming carbonyl

https://doi.org/10.5194/egusphere-2025-3845
Preprint. Discussion started: 4 December 2025


compounds, which act as major radical sources in $O_3$ production (Gillman et al., 2013; Edwards et al., 2014; Field et al., 2015).

The contribution of different NMOC groups to the $O_3$ production rate remained largely unchanged after incorporating heterogeneous chemistry in the box model simulation using MCMv331, consistent with the explanation provided in Section 3.2 (Fig. S5). Figure S9 shows that a 50% decrease in the mixing ratio of each NMOC group resulted in similar magnitudes of change in $O_3$ production rate, but in the opposite direction.

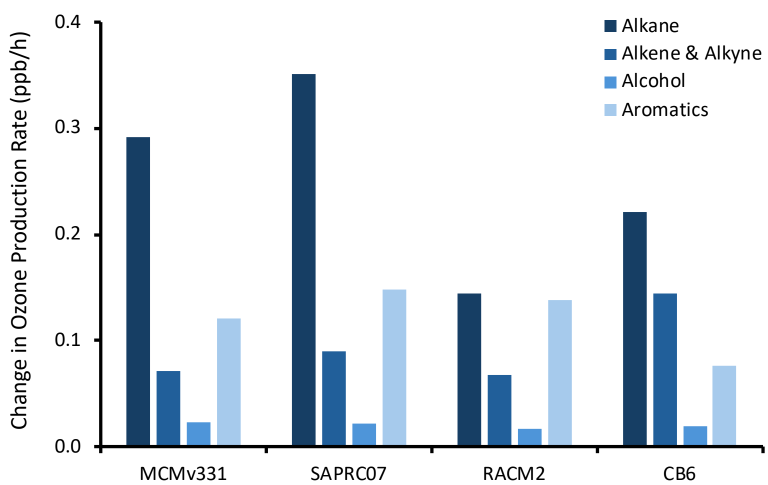


**Figure 7: Sensitivity of hydrocarbons to $O_3$ production rate. The bars represent the changes in $O_3$ production rate from the base model due to the increase in hydrocarbon initial mixing ratio by 50%.**

### *3.5 Budget Analysis of Ozone, HOx, and Carbonyl Species Across Four Chemical Mechanisms (MCMv3.3.1, SAPRC07, RACM2, and CB6)*

The ozone budget on Day 4 shows a consistent pattern across all four mechanisms (Tables S8.1–S8.4). Ozone production is controlled almost entirely by the reaction between ground-state oxygen atoms and molecular oxygen, contributing 99–100% of total formation, while reactions involving organic peroxy radicals and $HO_2$ contribute less than 0.01%. Ozone loss is driven mainly by photolysis, which accounts for 75–78% of total removal, followed by the reaction of NO with $O_3$, which contributes 18–21%.

A similar level of consistency appears in the HOx budget (Tables S9.1–S9.4). The largest source of HOx in all mechanisms is the decomposition of peroxynitric acid, contributing 23–38% of total production, with additional HOx formed through the oxidation

https://doi.org/10.5194/egusphere-2025-3845
Preprint. Discussion started: 4 December 2025


or photolysis of organic species. HOx loss is dominated by the reaction of $HO_2$ with $NO_2$, which contributes 25–40%, while reactions of OH with hydrocarbons contribute another 5–30%.

Carbonyl chemistry also follows a clear pattern across mechanisms (Tables S10.1–S10.4). Formaldehyde is formed mainly through reactions of methyl peroxy radicals and other organic peroxy radicals with NO, contributing 55–60% of total formation in MCMv3311, SAPRC07, and RACM2, and 36% in CB6. Its loss is controlled mostly by photolysis, which removes 85–90%, while OH oxidation contributes 10–12%. Acetaldehyde production is dominated by reactions involving ethyl peroxy radicals and larger peroxy radicals, accounting for 75–98% depending on the mechanism. Acetaldehyde loss is also dominated by OH, contributing 80–87%, while photolysis accounts for 10–17%. In CB6, the ketone species (KET) plays a larger role than in the other mechanisms. Nearly all KET formation (about 99%) comes from the oxidation of larger VOCs, and it is removed entirely by a single decay pathway. Overall, the carbonyl budgets show a consistent chemical pattern in which peroxy–NO reactions drive formation, while photolysis and OH oxidation dominate removal.

## 4. Conclusion

This box model study highlights formaldehyde as the most important carbonyl driving wintertime $O_3$ production in the Uinta Basin, followed by acetaldehyde, as consistently identified across the MCMv331, RACM2, and SAPRC07 mechanisms. Several NMOC groups contributed to formaldehyde formation, with alkanes showing the strongest influence on the production of other carbonyls. Alkanes also emerged as the dominant contributors to $O_3$ production, followed by aromatics, particularly in the MCMv331 and SAPRC07 simulations. The inclusion of heterogeneous chemistry showed limited impact on NMOC contributions, suggesting that the main chemical pathways remain robust under winter conditions in the Uinta Basin (Fig. S4 and S5). Among the lumped mechanisms, SAPRC07 performed best in representing the chemistry of winter $O_3$ formation, while CB6 may be suitable for pollutant estimation but lacks the detail needed to understand the chemical process. This study provides a useful framework for evaluating and selecting appropriate chemical mechanisms under specific seasonal and emission conditions. The results also underline the key role of alkanes and aromatics in oil and gas activities in winter $O_3$ formation, supporting the need for targeted emission reduction strategies.

**Code availability:** The F0AM Box model script can be provided by the corresponding author upon request.

**Data availability:** Measurement data used in this study are available at https://www.usu.edu/binghamresearch/data-access.

**Author contribution:** SL and LD planned the overall research framework and study objectives. LD conducted all atmospheric chemistry simulations and data processing. LD prepared the initial manuscript draft, including figures and interpretation of model results. SL provided critical revisions, contributed to the interpretation of findings, and supervised the entire project.

**Competing interests:** The authors declare that they have no conflict of interest.

https://doi.org/10.5194/egusphere-2025-3845
Preprint. Discussion started: 4 December 2025


**Acknowledgement:** We thank Huy Tran from the Center for Environmental Modeling for Policy Development at the University of North Carolina and RAMBOLL for providing the species mapping information. We also thank Pamela Gardner, Project Development Specialist at the Bingham Research Center, Utah State University, for reviewing and editing the grammar, spelling, and formatting. The authors also used ChatGPT for grammar editing.

**Financial support:** Funding for this work was provided by Uintah Special Service District 1 and the Utah State Legislature. Additional funding for student support was provided by an endowment from the Anadarko Petroleum Corporation.

**References**

1. Ashmore, M. R.: Assessing the future global impacts of ozone on vegetation, *Plant Cell Environ.*, **28**, 949–964, https://doi.org/10.1111/j.1365-3040.2005.01341.x, 2005.
2. Barnes, P. W., Williamson, C. E., Lucas, R. M., Robinson, S. A., Madronich, S., Paul, N. D., and Zepp, R. G.: Ozone depletion, ultraviolet radiation, climate change, and prospects for a sustainable future, *Nat. Sustain.*, **2**, 569–579, https://doi.org/10.1038/s41893-019-0314-2, 2019.
3. Bloss, C., Wagner, V., Jenkin, M. E., Volkamer, R., Bloss, W. J., Lee, J. D., and Pilling, M. J.: Development of a detailed chemical mechanism (MCMv3.1) for the atmospheric oxidation of aromatic hydrocarbons, *Atmos. Chem. Phys.*, **5**, 641–664, https://doi.org/10.5194/acp-5-641-2005, 2005.
4. Carbajo, P. G., Smith, S. C., Holloway, A. L., Smith, C. A., Pope, F. D., Shallcross, D. E., and Orr-Ewing, A. J.: Ultraviolet photolysis of HCHO: absolute HCO quantum yields by direct detection of the HCO radical photoproduct, *J. Phys. Chem. A*, **112**, 12437–12448, https://doi.org/10.1021/jp8070508, 2008.
5. Carter, W. P. and Seinfeld, J. H.: Winter ozone formation and VOC incremental reactivities in the Upper Green River Basin of Wyoming, *Atmos. Environ.*, **50**, 255–266, https://doi.org/10.1016/j.atmosenv.2011.12.025, 2012.
6. Carter, W. P.: Development of the SAPRC-07 chemical mechanism, *Atmos. Environ.*, **44**, 5324–5335, https://doi.org/10.1016/j.atmosenv.2010.01.026, 2010.
7. Chen, T., Xue, L., Zheng, P., Zhang, Y., Liu, Y., Sun, J., and Wang, W.: Volatile organic compounds and ozone air pollution in an oil production region in northern China, *Atmos. Chem. Phys.*, **20**, 7069–7086, https://doi.org/10.5194/acp-20-7069-2020, 2020.
8. Crounse, J. D., Nielsen, L. B., Jørgensen, S., Kjaergaard, H. G., and Wennberg, P. O.: Autoxidation of organic compounds in the atmosphere, *J. Phys. Chem. Lett.*, **4**, 3513–3520, https://doi.org/10.1021/jz4019207, 2013.
9. Edwards, P. M., Brown, S. S., Roberts, J. M., Ahmadov, R., Banta, R. M., de Gouw, J. A., and Zamora, R.: High winter ozone pollution from carbonyl photolysis in an oil and gas basin, *Nature*, **514**, 351–354, https://doi.org/10.1038/nature13767, 2014.
10. Edwards, P. M., Young, C. J., Aikin, K., de Gouw, J., Dubé, W. P., Geiger, F., and Brown, S. S.: Ozone photochemistry in an oil and natural gas extraction region during winter: simulations of a snow-free season in the Uintah Basin, Utah, *Atmos. Chem. Phys.*, **13**, 8955–8971, https://doi.org/10.5194/acp-13-8955-2013, 2013.

https://doi.org/10.5194/egusphere-2025-3845
Preprint. Discussion started: 4 December 2025


11. Field, R. A., Soltis, J., McCarthy, M. C., Murphy, S., and Montague, D. C.: Influence of oil and gas field operations on spatial and temporal distributions of atmospheric non-methane hydrocarbons and their effect on ozone formation in winter, *Atmos. Chem. Phys.*, **15**, 3527–3542, https://doi.org/10.5194/acp-15-3527-2015, 2015.
12. Filippidou, E. C. and Koukouliata, A.: Ozone affects the respiratory system, *Prog. Health Sci.*, **1**, 144–155, 2011.
13. Gilman, J. B., Lerner, B. M., Kuster, W. C., and de Gouw, J. A.: Source signature of volatile organic compounds from oil and natural gas operations in northeastern Colorado, *Environ. Sci. Technol.*, **47**, 1297–1305, https://doi.org/10.1021/es304119a, 2013.
14. Goliff, W. S., Stockwell, W. R., and Lawson, C. V.: The regional atmospheric chemistry mechanism, version 2, *Atmos. Environ.*, **68**, 174–185, https://doi.org/10.1016/j.atmosenv.2012.11.038, 2013.
15. Heard, D. E., Carpenter, L. J., Creasey, D. J., Hopkins, J. R., Lee, J. D., Lewis, A. C., and Emmerson, K. M.: High levels of the hydroxyl radical in the winter urban troposphere, *Geophys. Res. Lett.*, **31**, L18112, https://doi.org/10.1029/2004GL020544, 2004.
16. Koss, A. R., de Gouw, J., Warneke, C., Gilman, J. B., Lerner, B. M., Graus, M., and Quinn, P. K.: Photochemical aging of volatile organic compounds associated with oil and natural gas extraction in the Uintah Basin, UT, during a wintertime ozone formation event, *Atmos. Chem. Phys.*, **15**, 5727–5741, https://doi.org/10.5194/acp-15-5727-2015, 2015.
17. Lapworth, A.: The morning transition of the nocturnal boundary layer, *Bound.-Layer Meteorol.*, **119**, 501–526, https://doi.org/10.1007/s10546-005-9046-0, 2006.
18. Levy, H.: Normal atmosphere: Large radical and formaldehyde concentrations predicted, *Science*, **173**, 141–143, https://doi.org/10.1126/science.173.3992.141, 1971.
19. Lew, M. M., Rickly, P. S., Bottorff, B. P., Reidy, E., Sklaveniti, S., Léonardis, T., and Stevens, P. S.: OH and $HO_2$ radical chemistry in a midlatitude forest: measurements and model comparisons, *Atmos. Chem. Phys.*, **20**, 9209–9230, https://doi.org/10.5194/acp-20-9209-2020, 2020.
20. Lin, J. C., Bares, R., Fasoli, B., Garcia, M., Crosman, E., and Lyman, S.: Declining methane emissions and steady, high leakage rates observed over multiple years in a western US oil/gas production basin, *Sci. Rep.*, **11**, 22291, https://doi.org/10.1038/s41598-021-01721-5, 2021.
21. Liu, Y., Li, J., Ma, Y., Zhou, M., Tan, Z., Zeng, L., and Zhang, Y.: A review of gas-phase chemical mechanisms commonly used in atmospheric chemistry modeling, *J. Environ. Sci.*, **123**, 522–534, https://doi.org/10.1016/j.jes.2022.10.031, 2023.
22. Lyman, S. and Tran, T.: Inversion structure and winter ozone distribution in the Uintah Basin, Utah, USA, *Atmos. Environ.*, **123**, 156–165, https://doi.org/10.1016/j.atmosenv.2015.10.067, 2015.
23. Lyman, S. N., Elgiar, T., Gustin, M. S., Dunham-Cheatham, S. M., David, L. M., and Zhang, L.: Evidence against rapid mercury oxidation in photochemical smog, *Environ. Sci. Technol.*, **56**, 11225–11235, https://doi.org/10.1021/acs.est.2c02224, 2022.
24. Lyman, S. N., Holmes, M. L., Tran, H. N., Tran, T., and O'Neil, T.: High ethylene and propylene in an area dominated by oil production, *Atmosphere*, **12**, 1, https://doi.org/10.3390/atmos12010001, 2020.

25. Maasakkers, J. D., Jacob, D. J., Sulprizio, M. P., Scarpelli, T. R., Nesser, H., Sheng, J. X., and Parker, R. J.: Global distribution of methane emissions, emission trends, and OH concentrations and trends inferred from an inversion of GOSAT satellite data for 2010–2015, *Atmos. Chem. Phys.*, **19**, 7859–7881, https://doi.org/10.5194/acp-19-7859-2019, 2019.
26. Mahrt, L.: The early evening boundary layer transition, *Q. J. R. Meteorol. Soc.*, **107**, 329–343, https://doi.org/10.1002/qj.49710745205, 1981.
27. Mansfield, M. L. and Hall, C. F.: A survey of valleys and basins of the western United States for the capacity to produce winter ozone, *J. Air Waste Manag. Assoc.*, **68**, 909–919, https://doi.org/10.1080/10962247.2018.1454356, 2018.
28. Mansfield, M. L. and Hall, C. F.: Statistical analysis of winter ozone events, *Air Qual. Atmos. Health*, **6**, 687–699, https://doi.org/10.1007/s11869-013-0204-0, 2013.
29. Mansfield, M. L. and Lyman, S. N.: Seasonal trends in the wintertime photochemical regime of the Uinta Basin, Utah, USA, *EGUsphere* [preprint], https://doi.org/10.5194/egusphere-2024-3114, 2024.
30. Mansfield, M. L. and Lyman, S. N.: Winter ozone pollution in Utah's Uinta Basin is attenuating, *Atmosphere*, **12**, 4, https://doi.org/10.3390/atmos12010004, 2020.
31. NASA Giovanni: The Bridge between Data and Science, available at: https://giovanni.gsfc.nasa.gov/giovanni/, last accessed: 2 May 2024.
32. Neemann, E. M., Crosman, E. T., Horel, J. D., and Avey, L.: Simulations of a cold-air pool associated with elevated wintertime ozone in the Uintah Basin, Utah, *Atmos. Chem. Phys.*, **15**, 135–151, https://doi.org/10.5194/acp-15-135-2015, 2015.
33. Ninneman, M., Lyman, S., Hu, L., Cope, E., Ketcherside, D., and Jaffe, D.: Investigation of ozone formation chemistry during the Salt Lake Regional Smoke, Ozone, and Aerosol Study (SAMOZA), *ACS Earth Space Chem.*, **7**, 2521–2534, https://doi.org/10.1021/acsearthspacechem.3c00235, 2023.
34. Nogueira, T., Dominutti, P. A., Fornaro, A., and Andrade, M. D. F.: Seasonal trends of formaldehyde and acetaldehyde in the megacity of São Paulo, *Atmosphere*, **8**, 144, https://doi.org/10.3390/atmos8080144, 2017.
35. Nozière, B. and Vereecken, L.: H-shift and cyclization reactions in unsaturated alkylperoxy radicals near room temperature: propagating or terminating autoxidation?, *Phys. Chem. Chem. Phys.*, **26**, 25373–25384, https://doi.org/10.1039/D4CP02718C, 2024.
36. Oltmans, S., Schnell, R., Johnson, B., Pétron, G., Mefford, T., and Neely III, R.: Anatomy of wintertime ozone associated with oil and natural gas extraction activity in Wyoming and Utah, *Elem. Sci. Anth.*, **2**, 000024, https://doi.org/10.12952/journal.elementa.000024, 2014.
37. Pang, X. and Mu, Y.: Seasonal and diurnal variations of carbonyl compounds in Beijing ambient air, *Atmos. Environ.*, **40**, 6313–6320, https://doi.org/10.1016/j.atmosenv.2006.05.044, 2006.
38. Rauk, A., Boyd, R. J., Boyd, S. L., Henry, D. J., and Radom, L.: Alkoxy radicals in the gaseous phase: β-scission reactions and formation by radical addition to carbonyl compounds, *Can. J. Chem.*, **81**, 431–442, https://doi.org/10.1139/v02-206, 2003.

39. Saunders, S. M., Jenkin, M. E., Derwent, R. G., and Pilling, M. J.: Protocol for the development of the Master Chemical Mechanism, MCM v3 (Part A): tropospheric degradation of non-aromatic volatile organic compounds, *Atmos. Chem. Phys.*, **3**, 161–180, https://doi.org/10.5194/acp-3-161-2003, 2003.
40. Seinfeld, J. H.: Urban air pollution: state of the science, *Science*, **243**, 745–752, https://doi.org/10.1126/science.243.4892.745, 1989.
41. Shareef, M., Cho, S., Lyder, D., Zelensky, M., and Heckbert, S.: Evaluation of different chemical mechanisms on $O_3$ and $PM_{2.5}$ predictions in Alberta, Canada, *Appl. Sci.*, **12**, 8576, https://doi.org/10.3390/app12178576, 2022.
42. Simpson, D., Arneth, A., Mills, G., Solberg, S., and Uddling, J.: Ozone—the persistent menace: interactions with the N cycle and climate change, *Curr. Opin. Environ. Sustain.*, **9**, 9–19, https://doi.org/10.1016/j.cosust.2014.07.008, 2014.
43. Soares, A. R. and Silva, C.: Review of ground-level ozone impact in respiratory health deterioration for the past two decades, *Atmosphere*, **13**, 434, https://doi.org/10.3390/atmos13030434, 2022.
44. Stockwell, W. R., Lawson, C. V., Saunders, E., and Goliff, W. S.: A review of tropospheric atmospheric chemistry and gas-phase chemical mechanisms for air quality modeling, *Atmosphere*, **3**, 1–32, https://doi.org/10.3390/atmos3010001, 2011.
45. United States Environmental Protection Agency (EPA): SPECIATE database browser 5.2 for air emission modeling, available at: https://www.epa.gov/air-emissions-modeling/speciate-0, last accessed: 2 May 2024.
46. Wang, Z., Ehn, M., Rissanen, M. P., Garmash, O., Quéléver, L., Xing, L., and Sarathy, S. M.: Efficient alkane oxidation under combustion engine and atmospheric conditions, *Commun. Chem.*, **4**, 18, https://doi.org/10.1038/s42004-020-00445-3, 2021.
47. Warneke, C., Geiger, F., Edwards, P. M., Dube, W., Pétron, G., Kofler, J., and Roberts, J. M.: Volatile organic compound emissions from the oil and natural gas industry in the Uintah Basin, Utah: oil and gas well pad emissions compared to ambient air composition, *Atmos. Chem. Phys.*, **14**, 10977–10988, https://doi.org/10.5194/acp-14-10977-2014, 2014.
48. Wilkes, H. (Ed.): *Hydrocarbons, oils and lipids: diversity, origin, chemistry and fate*, Handbook of Hydrocarbon and Lipid Microbiology, Springer, https://doi.org/10.1007/978-3-319-90569-3, 2020.
49. Wolfe, G. M., Marvin, M. R., Roberts, S. J., Travis, K. R., and Liao, J.: The Framework for 0-D Atmospheric Modeling (F0AM) v3.1, *Geosci. Model Dev.*, **9**, 3309–3319, https://doi.org/10.5194/gmd-9-3309-2016, 2016.
50. Xiong, Y., Chai, J., Mao, H., Mariscal, N., Yacovitch, T., Lerner, B., and Huang, Y.: Examining the summertime ozone formation regime in Southeast Michigan using MOOSE ground-based $HCHO/NO_2$ measurements and F0AM box model, *J. Geophys. Res.-Atmos.*, **128**, e2023JD038943, https://doi.org/10.1029/2023JD038943, 2023.
51. Yang, J., Zeren, Y., Guo, H., Wang, Y., Lyu, X., Zhou, B., and Zhang, G.: Wintertime ozone surges: the critical role of alkene ozonolysis, *Environ. Sci. Ecotechnol.*, **22**, 100477, https://doi.org/10.1016/j.ese.2024.100477, 2024.
52. Yarwood, G., Jung, J., Whitten, G. Z., Heo, G., Mellberg, J., and Estes, M.: Updates to the Carbon Bond mechanism for version 6 (CB6), in: *Proceedings of the 9th Annual CMAS Conference*, Chapel Hill, NC, USA, 11–13 October 2010.

https://doi.org/10.5194/egusphere-2025-3845
Preprint. Discussion started: 4 December 2025


53. Zaveri, R. A. and Peters, L. K.: A new lumped structure photochemical mechanism for large-scale applications, *J. Geophys. Res.-Atmos.*, **104**, 30387–30415, https://doi.org/10.1029/1999JD900876, 1999.